Solid-solid crystal transitions (δ to α) in poly (hexamethylene carbonate) and poly (octamethylene carbonate)

Ricardo A. Pérez-Camargo[1], Guoming Liu[1,2], Leire Meabe[3], Ying Zhao[1,2], Haritz Sardon[3], Dujin Wang[1,2], and Alejandro J. Müller[3,4*]*

[1]Beijing National Laboratory for Molecular Sciences, CAS Key Laboratory of Engineering Plastics, Institute of Chemistry, Chinese Academy of Sciences, Beijing, 100190, China.

[2]University of Chinese Academy of Sciences, Beijing 100049, China

[3]POLYMAT and Department of Polymers and Advanced Materials: Physics, Chemistry and Technology, Faculty of Chemistry, University of the Basque Country UPV/EHU, Donostia-San Sebastián, 20018, Spain.

[4]IKESBASQUE, Basque Foundation for Science, Plaza Euskadi 5, Bilbao, 48009 Spain.

*Corresponding authors: gmliu@iccas.ac.cn and alejandrojesus.muller@ehu.es

For Table of Contents use Only

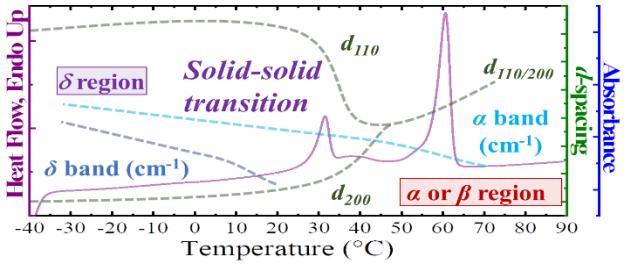

ABSTRACT

Poly (hexamethylene carbonate) (PC6) and poly (octamethylene carbonate) (PC8) were studied under different crystallization conditions. Using differential scanning calorimetry (DSC), a new solid-solid transition, denoted α to δ transition, was detected at low temperatures (<RT) in both PC6 and PC8 samples. The α to δ transition was represented by exothermic (*i.e.*, α to δ) (−6 °C (PC6) and −20 °C (PC8)) and endothermic peaks (*i.e.*, δ to α) (15 °C (PC6) and 28 °C (PC8)), during cooling and heating DSC scans, respectively. Isothermal tests revealed that this solid-solid transition depends on the specific thermal history, since it is not observed at isothermal temperatures higher than room temperature. Still, it is detected in the subsequent cooling and heating scans. Wide-angle X-ray scattering (WAXS) and Fourier-transform infrared spectroscopy (FT-IR) experiments were performed at identical conditions to those by DSC. WAXS experiments showed lower *d*-spacings in the δ phase than in the α one, corresponding to a unit cell shrinkage, explained by a more efficient packing of the methylene groups in the δ phase. The δ phase is also characterized, according to FT-IR experiments, by more ordered conformation of the methylene groups (*i.e.*, reflected in the appearance of a new absorption band) compared to the less ordered conformation in the α phase.

Keywords: aliphatic linear polycarbonates, solid-solid transitions, Brill-like transition, ordered and disordered conformations, unit cell shrinkage

1. Introduction

Aliphatic polycarbonates (PCs) are attracting a growing interest among biodegradable polymers since they show attractive chemical and physical properties and excellent biocompatibility and nontoxicity.[1-5] PCs show unique degradation since they can degrade by surface erosion without producing acid compounds.[6-8] Moreover, they also exhibit high ionic conductivity, good electrochemical stability, and high lithium transfer number.[9] As a result, PCs are suitable to meet demands in agriculture and packaging applications,[10] medical applications (*e.g.*, biomedicine and pharmaceutics)[11, 12] and solid polymer electrolytes.[9]

Traditionally, the repeating length of PCs (n_{CH2}) was limited by the synthetic route of ring-opening polymerization (*e.g.*, the size of the ring).[2, 9, 13] Nowadays, PCs can be obtained with different n_{CH2} numbers and without potentially toxic impurities by organocatalysis, allowing the adjustment of physical properties in a broader range. In a preceding work,[13] we studied PCs in the range of n_{CH2}= 6 to 12 and we were able to identify an even-odd effect. The even-odd effect was limited to n_{CH2}=6 to 9, with even samples (n_{CH2}=6 and 8) showing a monoclinic unit cell and the odd ones an orthorhombic one. As the n_{CH2} values increased, the even-odd effect was saturated for n_{CH2}=10 to 12. In this region, both even and odd samples showed an orthorhombic unit cell, and a PE-like dominated conformation, due to the weakening of the carbonyl group influence as n_{CH2} values increased.

Another interesting feature of PCs, specifically for poly (octamethylene carbonate) (PC8) was reported by Zhao et al.[14] They found that PC8 shows a reversible crystal-crystal transition (a crystalline phase is transformed into another crystalline phase without entering an isotropic liquid phase[15]), in analogy to the Brill transition in the nylon family.[16-25] The Brill transition can be considered as a first-order transition but with a second-order character (*i.e.*, it occurs

gradually and continuously in a wide range of temperature, independently of the molecular weight[26]).[23] It shows a hysteresis effect,[27] depending on the crystallization condition and thermal history,[28, 29] and its main characteristic is the merging of the two main X-ray reflections (intersheet and intrasheet interstem distances[23]) into a single one, with a *d*-spacing of 0.42 nm.

Different interpretations have been proposed to explain the Brill transition, from forming a pseudohexagonal arrangement to the disorder of methylene groups and recently pleated/rippled sheet structures. Even though the pseudohexagonal arrangement is found in nylon 6,6, other nylons (that show the Brill transition) have triclinic and monoclinic unit cells.[30, 31] Thus, alternatively it has been proposed that the origin of the transition is related to higher mobility or disorder of methylene groups,[18, 19, 26] or the aliphatic part, that leads to a new packing, or to a disruption of the initial hydrogen bonds to form new interactions.[27] In this new phase, *i.e.*, Brill transition region, the intermolecular hydrogen bond strength is weakening.[18] Recently, a new approach that recognizes the pleated/rippled sheet structures (*i.e.*, conformational isomers[23, 24]) has been proposed by Lotz.[23] According to this approach, the Brill transition is the sum of different processes, involving the generation of pleated and/or rippled sheet structures, its transformation to sheets (intrasheet process), and finally, the formation of temporary intersheet hydrogen bonds (under favorable conditions), leading to the characteristic reflection at 0.42 nm.[23]

The 0.42 nm characteristic reflection (*i.e.*, named as Brill form or β-phase) was also found in PC8[14] and poly (hexamethylene dithiocarbonate) (PDC-6).[32, 33] For PC8, Zhao et al.[14] designed a thermal protocol, performing an isothermal crystallization, at 50 °C (*i.e.*, to detect the β phase), followed by a cooling scan to 25 °C, and a subsequent heating scan to 80 °C (*i.e.*, to detect the α phase at T < 50 °C (Note that in the α phase more than two reflections are detected)). An

exothermic peak was found at ~42 °C during the cooling scan. This peak was related to the β to α transition. The subsequent heating shows the process reversibility since an endothermic peak at ~45 °C, related to the α to β transition, was found. This experiment was also reproduced during FT-IR and WAXS experiments, finding that the α phase is present at low temperatures (<42 °C) and shows *trans*-dominated conformation, strong dipole-dipole interactions between carbonyl groups, and a monoclinic unit cell. On the other hand, the β (*i.e.*, Brill transition region) phase of PC8 present at high temperatures (>42 °C) shows a *trans/gauche* coexistence, weakening the dipole-dipole interactions between the carbonyl groups and a monoclinic unit cell. The evidence found by Zhao et al.[14] to explain the Brill-like transition is in line with those found in the nylon family.[19, 26] However, it should be noted that the exact nature of the Brill transition is still elusive, and its nature is still debated.[23]

Zhao et al.[32] substituted the carbonate groups of a poly (hexamethylene carbonate) (PC6) by dithiocarbonate groups to obtain a PDC-6. In this way, a stronger Brill transition was obtained. The Brill transition in PDC-6 was also reported by Berti et al.[33] They found that the analogous PC6 does not show any solid-solid transition because sulfur atoms have lower electronegativity than oxygen atoms, and hence there are weaker polar inter-and intramolecular interactions in PC6 as compared to PDC-6.[33] It is worth noting that solid-solid transitions are not reported in other works related to PC6 samples.[34]

Our previous work pointed out that both PC6 and PC8 samples show atypical exothermic and endothermic transitions that might be related to solid-solid transformations.[13] These transitions were detected during non-isothermal differential scanning calorimetry (DSC) experiments, and further studies were needed to understand their origin. In the case of the PC8, in this work, we not only corroborate the found Brill transition reported by Zhao et al.,[14] but also

we report a novel different transition at lower temperatures.

In this work, we carefully study the origin of the solid-solid transitions mentioned above, in PC6 and PC8 samples, through a systematic characterization that includes performing non-isothermal and isothermal DSC experiments. *In-situ* Wide-angle X-ray Scattering (WAXS) and Fourier-transform infrared spectroscopy (FT-IR) experiments were performed to understand the origin of this new transition in PC6 and PC8 samples, namely the α to δ transition.

2. EXPERIMENTAL

2.1. Materials

Both poly (hexamethylene carbonate) (PC6) and poly (octamethylene carbonate) (PC8) were prepared by conventional polycondensation of aliphatic diols and dimethyl carbonate following a previously established protocol. Briefly, the melt-polycondensation was performed using 4-dimethylaminopyridine (DMAP) organocatalyst in two steps at 130 and 180 °C under vacuum. For more details, see references 9 and 35.

2.2. Differential Scanning Calorimetry (DSC) Experiments

A Perkin Elmer DSC, model 8500, connected to a controlled liquid nitrogen accessory (CLN2), was employed to perform the DSC experiments. The instrument was calibrated with indium and zinc standards and was operated with a constant flow (20 mL/min) of ultrapure N_2. All the samples were encapsulated in aluminum DSC pans. In all the cases, a sample weight of *circa* 5 mg was used. The employed thermal protocols are described below.

Non-isothermal DSC tests

The samples were heated, as received, from room temperature (RT) to *T* (*i.e.*, the

temperature of erasing thermal history), to register the first heating scan. The samples were maintained at *T* for 3 min, and then were cooled until −40 °C, and maintained at that temperature for 1 min. The second heating scan was recorded by heating the samples from −40 °C to *T*. All the employed scanning rates were 20 °C/min.

Isothermal DSC experiment followed by non-isothermal tests

To perform isothermal crystallization tests, we first determined the minimum crystallization temperature ($T_{c,\,min}$) that can be employed without sample crystallization during cooling from the melt to the isothermal crystallization temperature (T_c) at a rate of 60 ºC/min and used it as the starting point of the isothermal experiments, as is recommended in the protocol reported by Lorenzo et al.[36]

The thermal history of the samples was erased at *T*, and then they were cooled at 60 °C/min until T_c ($T_c \geq T_{c,min}$), and held at this point enough time to reach a complete crystallization, registering the isothermal crystallization behavior of the sample. Normally, after the isothermal step, the sample is heated from T_c to record its subsequent melting.

In this work, we introduced, after the isothermal step, a modification of the above-described protocol. The aim of this modification is to amplify the signal of the crystal-crystal transition, following Zhao et al.[14] Thus, after applying isothermal steps at three different selected T_c, we perform subsequent cooling and heating scans, at 20 °C/min and therefore imprinted different thermal histories in the material. The sample was cooled down to 25 and also to −40 °C for the PC6, and to 10 and −40 °C for the PC8. In both cases, the temperature was held for 1 min. During the cooling and heating scans, we can record any extra transition on the sample after the isothermal crystallization.

2.3. Wide-angle X-ray scattering (WAXS) experiments

WAXS experiments were performed *in-situ* at the beamline 1W2A of Beijing Synchrotron Radiation Facility (BSRF). The sample-to-detector distance was 140.9 mm, the pixel size 172x172 μm^2, and a Pilatus 1M detector (resolution 981 x 1043 pixels) was employed. The wavelength was 1.54 Å. The thermal protocols described in Section 2.2 were reproduced in a Linkam TST350 hot stage, taking WAXS patterns simultaneously with an exposure time of 10 seconds.

2.4. FT-IR

A Nicolet 6700 Fourier transform infrared (FT-IR) spectrometer of Thermo Fisher connected to a Linkam FTIR 600 hot stage coupled to a liquid nitrogen supply was employed. The PC6 and PC8 samples were film-cast in chloroform (by dissolving 5 mg of sample in 1 mL of $CHCl_3$) onto potassium bromide (KBr) plates. The described protocols in Section 2.2 were reproduced in the hot stage. We recorded FT-IR spectrum using holding times of 1 min and with a resolution of 4.0 cm^{-1} at each selected temperature and coaddition of 32 scans per spectrum.

3. RESULTS AND DISCUSSION

The PC6 and PC8 samples were studied with different crystallization conditions, created with non-isothermal and isothermal experiments. The applied thermal protocols were analyzed with DSC, X-rays, and FT-IR experiments, and their results are shown below.

3.1. Non-isothermal experiments

Figure 1 shows the DSC cooling (Figure 1a) and subsequent heating (Figure 1b) scans for PC6 and PC8, performed with cooling and heating rates of 20 °C/min.

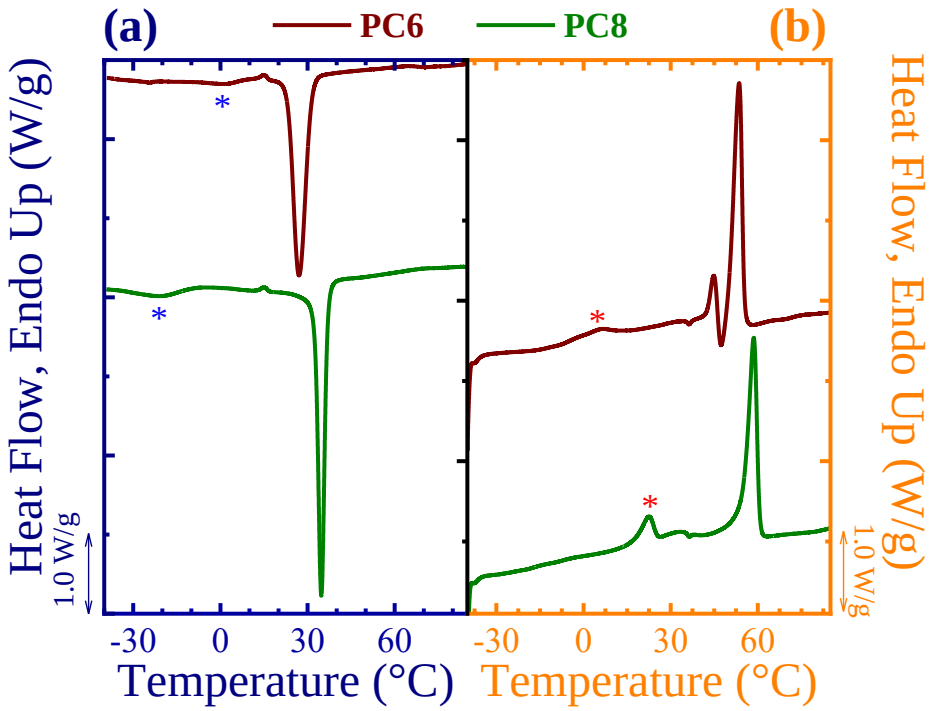

Figure 1. Non-isothermal DSC (a) cooling and (b) second heating scans performed for PC6 and PC8. The asterisk (*) indicates the position of the new transition found during the cooling and heating scans.

Figure 1 shows that besides the usually reported thermal transitions (*i.e.*, crystallization and melting temperatures) for PC6 and PC8,[13] there are exothermic and endothermic peaks (see the asterisk in Figure 1) below RT, detected during cooling, at −6 °C (PC6) and −20 °C (PC8), and second heating scans, at 15 °C (PC6) and 28 °C (PC8). None of these transitions are present during the first heating scan, as shown in Figure S1 on the SI. Thus, they are transitions that depend on the specific thermal history applied, and their origin is discussed below.

For PC8, a crystal-crystal transition has been already reported by Zhao et al.[14] They found an α to β (*i.e.*, Brill-like region) transition, similar to the Brill transition, during cooling and heating scans, at 10 °C/min, after isothermally crystallizing the sample at 50 °C. They

detected an exothermic peak at ~42 °C, and an endothermic peak at 45 °C during the cooling and heating scans, respectively. These peaks were assigned to the β to α (*i.e.*, cooling), and α to β (*i.e.*, heating) transitions, respectively.

In this work, we study new transitions below RT (besides the already reported α to β transition in the PC8) in both PC6 and PC8. As far as the authors are aware, this is the first time these transitions are reported, and their origin studied. In our previous work,[13] only non-isothermal experiments (with DSC, X-rays, and FT-IR techniques) were performed on these samples but we focused on the even-odd effect of melting temperature. In this new contribution, we have performed a series of different experiments designed to elucidate the origin of these novel low temperature solid-solid transitions.

3.2.Detection of transitions after isothermal test

The protocol employed by Zhao et al.[14] (*i.e.*, non-isothermal scans after isothermal crystallization) was adapted to our samples. In this case, after the isothermal crystallization test, the samples were cooled until different temperatures (*i.e.*, between 25 and −40 °C). Figure 2 shows the cooling (to −40 and 25 °C) and heating scans after the isothermal crystallization of the samples at selected T_c values (*i.e.*, 42 °C (PC6) and 44 °C (PC8)), for PC6 (Figures 2a and b) and PC8 (Figures 2c and d). The samples were also isothermally crystallized at other temperatures, as is shown in Figure S2.

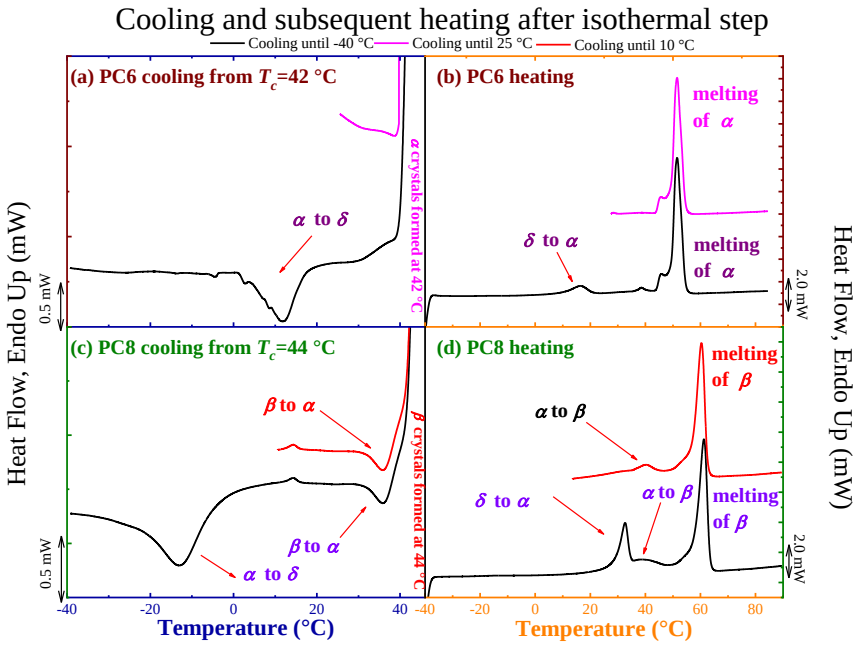

Figure 2. (a, c) cooling and (b, d) heating scans at 20 °C/min after isothermally crystallizing the samples at the indicated crystallization temperatures for PC6 (Figures 2a and b) and PC8 (Figures 2c and d) samples. The different transitions are indicated with arrows.

Figures 2a and b show the cooling and heating scans for PC6. If the sample is cooled from its T_c value (*i.e.*, 42 ºC) until 25 °C, there is no exothermic peak, and the subsequent heating shows a main melting peak of the isothermally crystallized crystals, denoted as α. But, if the sample is cooled from its T_c value (*i.e.*, 42 ºC) until −40 °C, it is detected an exothermic peak (~12 °C). This exothermic peak is due to a new transition that we have denoted, α to δ transition (see that this peak is similar to the asterisk in Figure 1). In the subsequent heating scan, the reverse of this transition occurs in an endothermic peak (~16 °C), denoted as δ to α, similar to the peak (see asterisk in Figure 1) detected during the non-isothermal experiments. Then, the α crystals formed during the isothermal crystallization step, melt, at exactly the same position as when the sample was cooled until 25 °C. This melting corresponds to the melting of the α

crystals.

For PC8 (Figure 2c and d), cooling either until 10 °C or −40 °C, evidences the β to α (exothermic peak) and the α to β (endothermic peak at low temperatures) transitions reported by Zhao et al.[14] When the sample was cooled to −40 °C, besides the transitions mentioned above, a new exotherm (~ −13 °C, even with higher area than the β to α peak), denoted as α to δ, and an endotherm (~33 °C), denoted as δ to α, appeared (note that these peaks are also detected in non-isothermal experiments, as we pointed out with an asterisk in Figure 1). These transitions have never been reported before. The reversibility and hysteresis of the δ to α transitions, of both PC6 and PC8, allows us to conclude that they correspond to solid-solid transitions at low temperatures. Below we investigate their origin.

For PC8, we confirm that the Brill-like transition (*i.e.*, α to β) increases as T_c increases (see Figure S2), as reported in the literature.[14, 17, 32] Interestingly, the α to δ transitions, for both PC6 and PC8 also increase with T_c. The transitions mentioned above are reflected in the WAXS and FT-IR experiments through shifts in the q positions of the main peaks and changes in the appearance of absorption bands. These changes are discussed below.

3.2.1 Real-time WAXS/After Isothermal experiments

The modified isothermal protocol performed with DSC was reproduced and applied in a hot stage, and at the same time, *in-situ* WAXS patterns were taken. As shown in Figures 3 and 4, the solid-solid transitions described above are related to a shift in the q positions of the main reflections. The most significant changes occur at the same temperatures detected by DSC (see Figure 2). The changes suggest different packing between the δ and the α phase.

The crystalline structure of PC6 has not been determined by using fiber patterns.

However, in our previous work,[13] we have estimated the unit cell parameters of PC6 considering its similarity with the known crystalline structure of its polycarbonate glycol analog.[37] Thus, PC6 can be indexed to a monoclinic unit cell with a=0.746 nm, b=0.631 nm, and α=60°, with its main peaks at q=14.3 nm^{-1} (2θ=20.1°) and 16.8 nm^{-1} (2θ=23.8°) (*i.e.*, d-spacing of 0.441 and 0.373 nm, respectively), corresponding to the *(110)* and *(200)* planes, respectively.

For PC8, Zhao et al.[14] determined that its α and β forms are both monoclinic. The α unit cell show parameters of a=0.77 nm, b=1.01 nm, c (fiber axis) =2.52 nm, and α=31.5°, and their main peaks at q=14.5 nm^{-1} (2θ=20.45°) and 16.4 nm^{-1} (2θ=23.14°) (*i.e.*, d-spacing of 0.430 and 0.380 nm, respectively) indexed to the *(110)* and *(200)* planes. The β form displays a larger a value (a=0.81 nm), but a smaller b dimension (b=0.89 nm) than the α form, leading to d-spacing= 0.41 nm, corresponding to the *(110)/(200)* planes. Also, the β form shows a c (chain axis)= 2.42 nm, and α= 31.9°.[14] In the β form, the only reflection is obtained at q=15.5 nm^{-1} (2θ=21.91°). Note that in references 14 and 37, the a-axis is defined as the unique axis; and the monoclinic angle is chosen to be lower than 90°. For the sake of clarity, below we analyzed the PC6 and PC8 samples, separately.

PC6 WAXS Analysis

Figure 3 shows WAXS patterns taken for PC6 during cooling (from T_c=42 to −40 °C (Figure 3a) and T_c=42 °C to 25 °C (Figure 3b)) and heating scans (from −40 to 85 °C (Figure 3c) and 25 to 85 °C (Figure 3d)) after the previous isothermal crystallization at 42 °C.

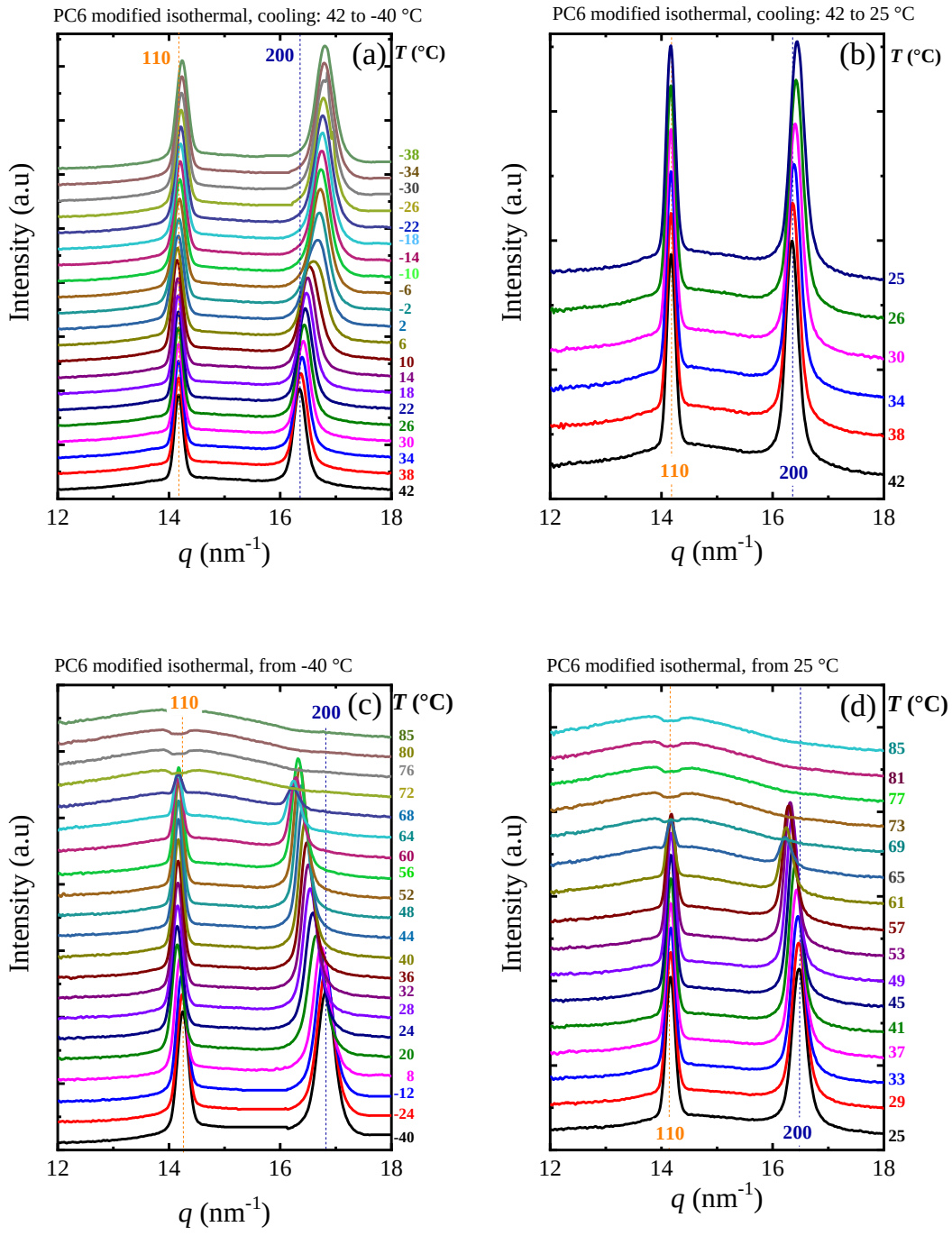

Figure 3. WAXS patterns, for PC6, taken during cooling: (a) 42 °C to −40 °C; (b) 42 °C to 25 °C; and subsequent heatings: (c) −40 °C to 85 °C; and (d) 25 to 85 °C. The vertical dashed lines indicate the *(110)* and *(200)* planes.

By comparing Figures 3a and c with Figures 3b and d, it is observed that the larger shifts in q occur below 25 °C, in line with the transition detected in Figures 2a and b, indicating that a new crystalline phase is formed below RT. The transition temperature is better observed when the d_{110} and d_{200} are plotted as a function of the temperature in Figure 4.

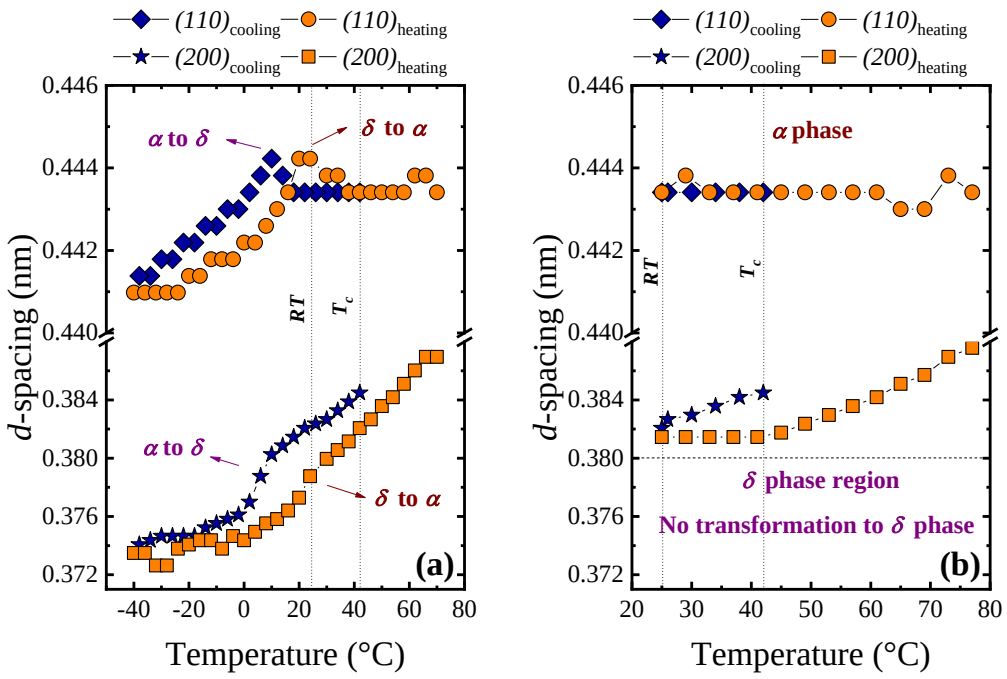

Figure 4. *d*-spacing evolution, for the main planes (PC6) as a function of temperature for (a) cooling: 42 °C to −40 °C and subsequent heating to 85 °C, and (b) cooling: 42 °C to 25 °C, and subsequent heating to 85 °C. In Figure a, the transitions are indicated with arrows. The vertical lines indicated the T_c and RT.

Figure 4 clearly illustrates that the found transitions depend on thermal history since there is a significant difference between cooling to −40 °C (Figure 4a) or cooling to 25 °C (Figure 4b), and their subsequent heatings, after the sample was isothermally crystallized at 42 °C.

Figure 4a shows that during cooling, the d_{110} remains unchanged or in an α phase until it

reaches ~10 °C. At this transition temperature, the *d*-spacing reaches a maximum and decreases, indicating the change to an δ form. At −40 °C, the d_{110} is lower compared to the d_{110} at 42 °C (*i.e.*, selected T_c), evidencing the differences between the α and δ forms. When the sample is heated, it is observed practically the same evolution but with a higher δ to α transition temperature, explained by hysteresis, as expected according to the DSC results. Such changes are not present (*i.e.*, only the α is present) when the sample is cooled to only 25 °C (see Figure 4b), indicating that the transition is promoted at $T < 25$ °C, *i.e.*, it depends on the thermal history.

The evolution of the d_{200} as a function of the temperature was also followed; see Figures 4a and b. In Figure 4a, during cooling, the d_{200} is continually decreasing, but such a decrease shows an acceleration at the indicated α to δ transition temperature. Then, lower changes of d_{200} as temperature decreases are registered. The heating process is similar, except for a higher temperature for the δ to α transition, characterized by a higher increase of the *d*-spacing, as expected.

In contrast, Figure 4b shows a slight decrease of d_{200} during cooling. Interestingly, in the subsequent heating, d_{200} remains unchanged from 25 to around 40 °C, and then increases at higher melting temperatures. Therefore, such an increase is related to the thermal expansion of the unit cell, instead of a solid-solid transition, as in Figure 4a. It is worth noting that the *d*-spacing evolution with temperature, is similar to the one found in d_{100} and $d_{010/110}$ before the Brill transition in different nylons (*e.g.*, PA26, PA46, and PA66[23]). Interestingly, the PDC-6 (same n_{CH2} as the PC6), which has stronger dipolar interactions, presents a Brill transition process,[32, 33] similar to the nylons.[23]

PC8 Analysis

As we showed in Figures 2c and d, PC8 has a complex behavior compared to PC6, due to the already known α to β transition (*i.e.*, Brill-like transition[14]). Figure 5 shows WAXS patterns for PC8 taken during the cooling from 44 °C (*i.e.*, selected isothermal temperature) to −40 °C (Figure 5a) and 44 °C to 10 °C (Figure 5b), and their subsequent heating from −40 to 90 °C (Figure 5c) and 10 to 90 °C (Figure 5d).

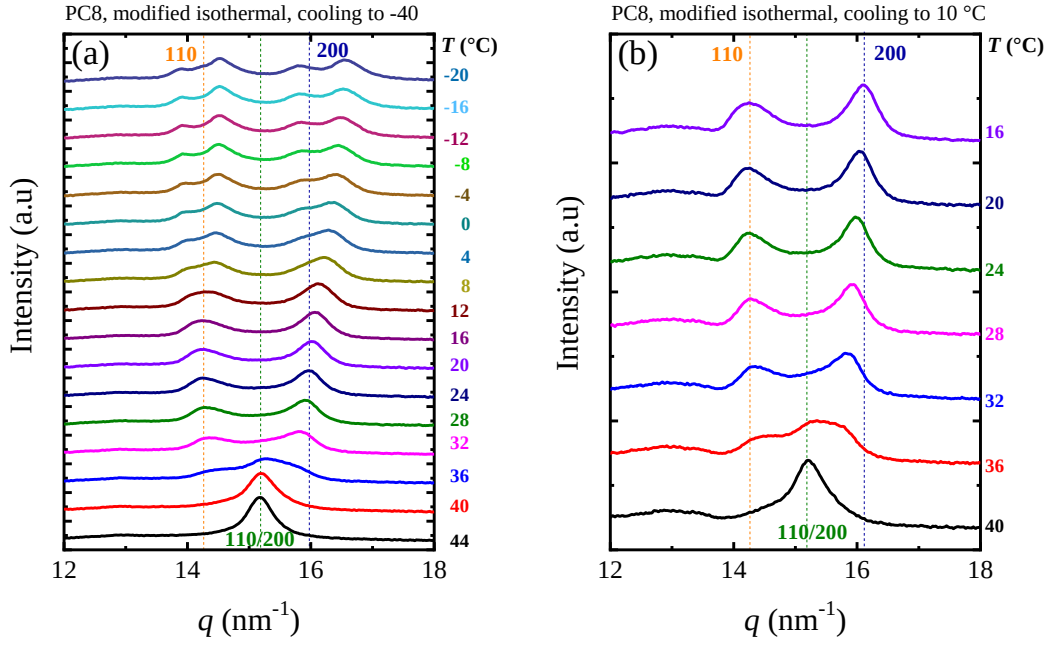

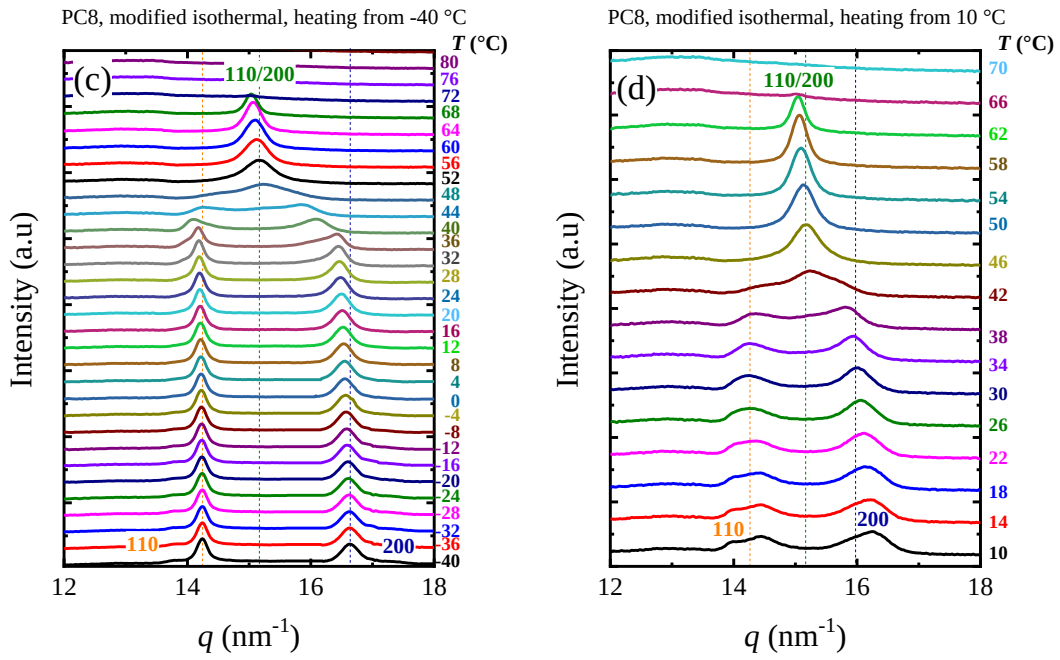

Figure 5. WAXS patterns, for PC8, taken during cooling: (a) 44 °C to −40 °C; (b) 44 °C to 10 °C; and subsequent heatings: (c) −40 °C to 90 °C; and (d) 10 to 90 °C. The vertical dashed lines indicate the *(110)* and *(200)* main planes, and the main signal of the *β*-phase (*i.e.*, Brill-like) indexed as (110)/(200) planes.

Figure 5 shows that the most evident change is the *α* to *β* transition, already reported by Zhao et al.[14] This transition occurs independently of the applied thermal protocol. As in PC6, below a certain temperature, in this case, 10 °C, there is a significant shift of the *q* values, especially for the *(200)* plane. Furthermore, at low temperatures, the development of shoulders is observed in the already broad reflections of the PC8. Although such features might be related to the *δ* phase, further crystallographic analysis is needed, which is outside the scope of the present work. Therefore, we will focus on the *d*-spacing analysis. The d_{110} and d_{200} have been followed

as a function of temperature, and plotted in Figure 6.

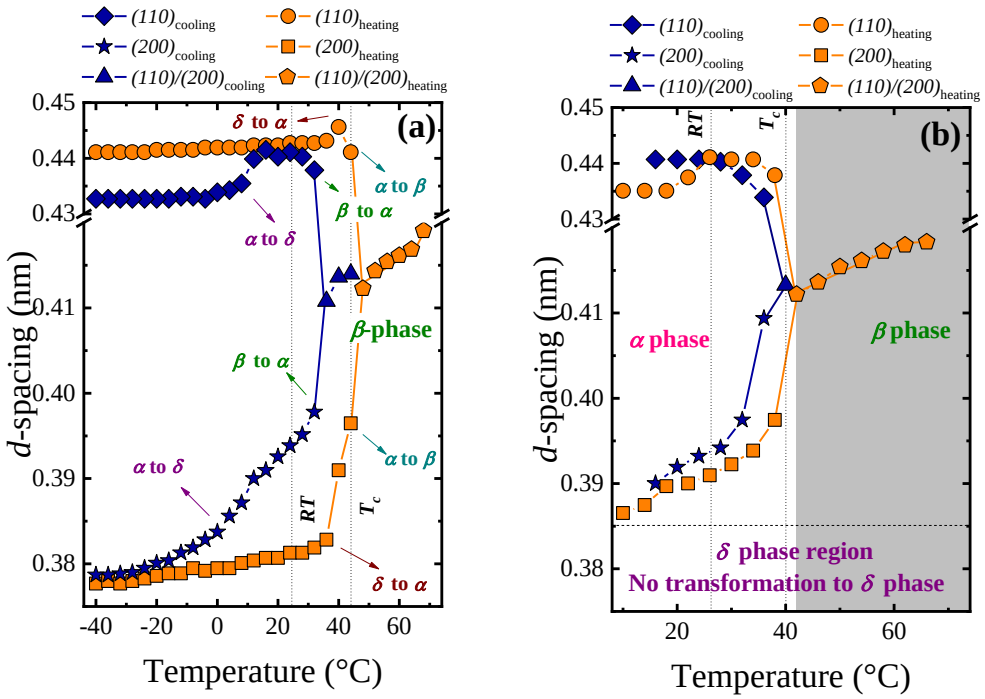

Figure 6. *d*-spacing evolution, for the main planes of PC8, as a function of temperature for (a) cooling: 44 °C to −40 °C and subsequent heating to 90 °C, and (b) cooling: 44 °C to 10 °C, and subsequent heating to 90 °C. In Figure a, the transitions are indicated with arrows, and in Figure b, the shadowed region indicates the β-phase. The vertical lines indicate T_c values and RT.

As for PC6, Figure 6 illustrates the thermal history dependance of the named, α to δ transition in PC8, which only appears when the sample is cooled up to −40 °C (Figure 6a). Note that this new transition is not present when the sample is cooled until 10 °C (Figure 6b).

If we follow the d_{200} during the cooling process, in Figure 6a, it is observed that after the isothermal crystallization at 44 °C, the sample maintain its β phase until ~ 32 °C, the temperature at which it changes to the α phase (characterized for presenting two diffraction peaks). At ~ 0 °C,

there is a change on the d_{200} slope (*i.e.*, the d_{200} starts to change slower), attributed to the α to δ transition. Then, the d_{200} reaches a stabilization at ~ −20 °C. The temperatures at which there are significant changes of the d_{200} values are in line with those detected in the DSC. In the case of the *(110)* planes, the changes are smaller.

Figure 6a also shows the evolution of the d_{200} during the heating process. In this case, the increase of both d_{200} and d_{110} is related to the δ to α transition at ~20 to 30 °C. In contrast, the α to β transition is characterized by a decrease of d_{110} and an increase of d_{200} at ~40 °C. The d_{110} and d_{200} converge in the β-phase. According to Lotz,[23] the Brill transition, in nylons, involves two different transitions: From the α phase to an intermediate pleated/rippled sheet structure, and from this structure to the Brill structure. Therefore, considering the structural similarities but different dipolar interactions between PCs and nylons, we can hypothesize that the two transitions found in this work are similar to the ones postulated by Lotz.[23]

To sum up, both PC6 and PC8 samples show a newly detected δ phase characterized by lower *d*-spacing (see Figures 4 and 6), evidencing smaller unit cell sizes than the α and β phases. This difference is attributed to a more compact structure for the δ phase. To understand the origin of such compactness, we performed *in-situ* FT-IR experiments.

3.2.2 Simultaneous FT-IR/After Isothermal experiments

The solid-solid transitions are related to crystal packing,[15] which is influenced by the conformation of the chains within the crystals. Hence, FT-IR is a suitable technique to understand the origin of the found transitions. Consequently, the different crystallization conditions, in this case, isothermal crystallization, were reproduced during FT-IR experiments.

The FT-IR experiments show that both PC6 and PC8 possess strong bands related to

carbonate and methylene group vibrations (see Figure S3), which were described in detail in our previous work.[13] In this work, for the characterization of the solid-solid transitions, we have studied the vibrations of methylene groups in *trans* and *gauche* conformation and also found newly bands (related to methylene groups) associated with the δ phase, The Brill transition analysis in nylons also focuses on methylene groups, specifically their disorder.

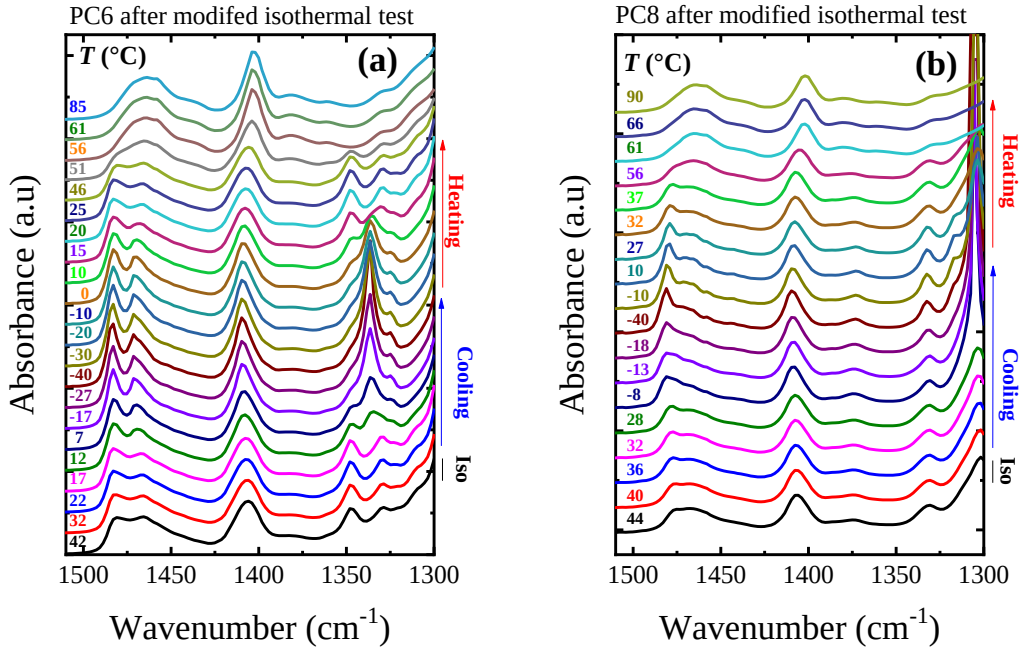

Figure 7. FT-IR spectra recorded during cooling and heating process after isothermal crystallization, at 42 °C (PC6) and 44 °C (PC8), for (a) PC6 and (b) PC8 in the CH_2-bending bands.

Figure 7 shows the IR spectra in the range from 1500 to 1300 cm^{-1} of both PC6 and PC8, during cooling and heating scans, after the isothermal crystallization. Those absorption bands of PC6 and PC8 correspond to vibrations of methylene groups in *gauche* (1460 cm^{-1}) and *trans* (1482 cm^{-1}) conformations, as described in our previous study.[13] As shown in Figure 8, the

relative intensity of these two bands (I_{1482}/I_{1460}) changes with the temperature.

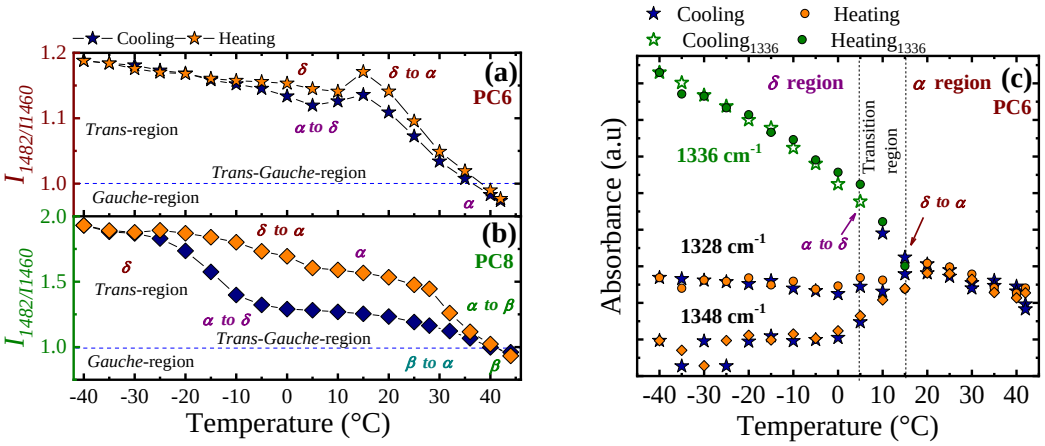

Figure 8. Variation of (a,b) I_{1482}/I_{1460} for (a) PC6 and (b) PC8 with temperature; and (c) variation of absorbance of different bands of the PC6, as a function of the temperature.

Figure 8 shows that after the isothermal step, both PC6 (Figure 8a) and PC8 (Figure 8b), have $I_{1482}/I_{1460} < 1.0$, which indicates coexistence of both *trans* and *gauche* conformations. Such *trans/gauche* conformation coexistence is characteristic of the β phase of PC8.[14] During the cooling process; the $I_{1482}/I_{1460}>1.0$ indicates a *trans*-dominated conformation. This change in the PC8 (see Figure 8b) is related to the β to α transition.[14] Below 25 °C, an increase in the I_{1482}/I_{1460} at the transition temperature, might indicate a higher dominance of the *trans* conformation in the new δ phase (see Figures 8a and b). Upon heating, the reversibility of the solid-solid transition is observed.

For PC6, Figure 7a shows that a new absorption band at 1336 cm^{-1} appears in the δ phase (~5 °C). Thus, in Figure 8c, we plot the evolution of the absorbance vs. temperature, for the bands at 1348, 1336, and 1328 cm^{-1}. Figure 8c shows the appearance of the bands at 1336 cm^{-1} (at ~5 °C) during cooling and its disappearance (at ~15 °C) during heating. Thus, such band is related to the α to δ transition (*i.e.*, cooling), and subsequent δ to α transition (*i.e.*, heating). The

above-described variation of the absorption bands is correlated with the conformational change of methylene groups during the solid-solid transition. Similar changes can be observed for the PC8 in this region at the transition temperatures. A band at ~1316 cm^{-1} appears (δ phase), and at the same time, the bands at ~ 1316 cm^{-1} and ~1301 cm^{-1} become intense and sharp. In this case, these two bands are difficult to analyze because of the saturation of the signal.

As far as the authors are aware, the IR bands mentioned above have never been reported for PCs. Therefore, further studies beyond the scope of this work are needed to understand the origin of these new bands. However, we found that the evolution of these bands resembled those found in nylons by Yoshioka et al.[18] A strong band at 937 cm^{-1}, related to the amide adjacent to the methylene group, becomes weaker when increasing temperature. Such a decrease in absorbance is attributed to the weakening of the hydrogen bond strength at the Brill transition. Additionally, as this band becomes weaker, other new weak bands appear due to the so-called progression bands of methylene segments.[18] In our case, at the δ phase, the carbonyl group interactions are strong, whereas, in the α phase, they start to get weak, as the different methylene groups become disordered, as evidenced by the broad bands and the appearance of new bands.

We have selected other regions in which strong changes, related to the solid-solid transitions, were detected. For PC6 (Figure 9a), we analyzed the absorption bands in the range of 780 to 700 cm^{-1}. This region gives an idea of the conformational disordering of the methylene segments,[18] since it is a part of the progression band series (rocking-twisting mode) of *n*-paraffins (n_{CH2}= 6 to 12).[38-40] For PC8, we selected the region of 980 to 900 cm^{-1} (Figure 9b). In Figures 9c and d, we plot the absorbance evolution of the main bands vs. temperature, for PC6 and PC8, respectively.

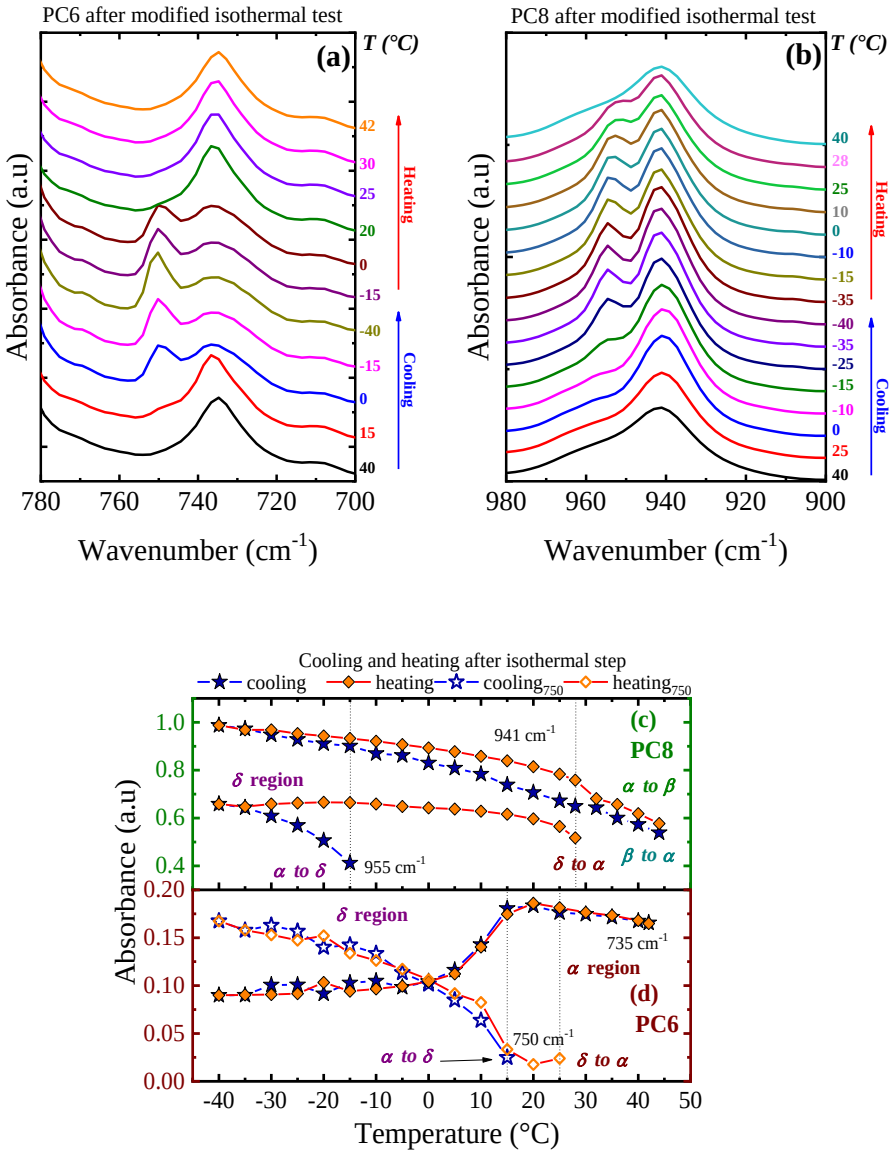

Figure 9. FT-IR spectra recorded during cooling and heating after isothermal crystallization at T_c= 42 °C (PC6) and 44 °C (PC8) for (a) PC6 in the range of 780 to 700 cm^{-1}, and (b) PC8 in the range of 980 to 900 cm^{-1}. In (c) (PC8) and (d) (PC6), the absorbance evolution of the found bands in (a) and (b) are plotted as a function of the temperature for (c) PC8 and (d) PC6. The vertical dotted lines indicate the α to δ and δ to α transitions, during cooling and heating, respectively.

Figure 9a shows that PC6 displays a single band (~735 cm^{-1}) at T > 25 °C (α phase), characteristic of its crystallization in a monoclinic unit cell. Upon cooling, at ~ 15 °C (δ phase, see Figure 7d), an additional band appears at ~750 cm^{-1} (see Figure 9a), and its absorbance gradually increases with temperature decreasing, while the band at ~ 735 cm^{-1} becomes weaker. The new band at ~750 cm^{-1} might indicate a different conformational arrangement for the δ phase. For nylons, it is reported in the range from 1100 to 800 cm^{-1} that there are two bands in the α phase, whereas, in the Brill transition, one of the bands disappears, indicating a *gauche* conformation dominance. Upon heating, the 750 cm^{-1} band disappearance at ~25 °C, demonstrated the reversibility (δ to α transition) of the solid-solid transition. It is worth noting that PC8 does not show such changes in the selected region.

Figures 7b and d show the PC8 related bands. A similar evolution to the one shown for PC6 was found. A band, at 941 cm^{-1}, characterizes the β and α phase, but at ~ −15 °C, an additional band, at 955 cm^{-1}, appears, indicating the transition to the δ phase. During the heating, this band disappears at T > 20 °C, as found by DSC.

Both PC6 and PC8 show that the α to δ transition is related to a transition between disordered methylene groups, in the α phase, to ordered ones. Such order is reflected in the appearance of new absorption bands. Upon heating, the reverse process occurs (δ to α transition). For PC8, an additional α to β transition (*i.e.*, Brill-like transition) was recorded. In contrast, PC6 does not reach a β phase, probably due to weaker dipole-dipole interactions. Stronger dipole-dipole interactions derivate in a Brill transition for PDC-6.[32, 33]

The results above reflect that the new solid-solid transition will be observable when the crystallization conditions involve low temperatures. The α to δ transition is characterized by decreased *d*-spacing, indicating a shrinkage in the unit cell due to a more efficient packing in the

δ phase. The efficient packing is also reflected in the FT-IR experiments. The appearance of extra bands indicates a more ordered conformation of the methylene groups in the δ phase than in the α phase.

4. CONCLUSIONS

In this paper we have found that independently of the crystallization conditions, PC6 and PC8 exhibit solid-solid transitions below room temperature that have never been reported in the literature. These solid-solid transitions were denoted α to δ transition. The transitions were found to be reversible. *In-situ* wide-angle X-ray scattering (WAXS) and Fourier-transformed infrared (FT-IR) experiments were employed to investigate the origin of these transitions. WAXS experiments revealed that the α to δ transition is related to a shift in the *d*-spacing at the same temperatures detected on the DSC. Such changes in the *d*-spacing are associated with the shrinkage of the unit cell due to different chain package. Thus, there is a more efficient package of the methylene groups in the δ phase (*i.e.*, low *d*-spacing) than in the α phase (*i.e.*, high *d*-spacing). The FT-IR experiments help explained the X-rays findings, since they evidenced that the transition goes from ordered (δ phase, characterized by extra absorption bands) to more disordered (α phase, characterized by the disappearance of the bands related to the δ phase) conformations.

ACKNOWLEDGMENTS

This work is supported by the National Key R&D Program of China (2017YFE0117800) and the National Natural Science Foundation of China (51820105005, 21922308, and 52050410327). We would like to thank the financial support provided by the BIODEST project; this project has received funding from the European Union's Horizon 2020 research and innovation programme under the Marie Sklodowska-Curie grant agreement no. 778092. This

work has also received funding from MINECO through project MAT2017-83014-C2-1-P and from Basque Government through grant IT1309-19. R.A.P.-C is supported by the China Postdoctoral Science Foundation (2020M670462). G.L. is grateful to the Youth Innovation Promotion Association of the Chinese Academy of Sciences (Y201908). We also thanks to the BSRF (beamline 1W2A).

Supporting Information

Additional DSC curves, including (a) first heating scan and (b) cooling and heating scan after isothermally crystallized the samples at different isothermal crystallization temperatures. FT-IR spectra for the complete (4000 to 700 cm^{-1}) range.

5. References

1. Su, W.; Feng, J.; Wang, H.-F.; Zhang, X.-Z.; Zhuo, R.-X. Controllable preparation of poly(alkylene carbonate)s and observation on their structure-related odd–even effect. *Polymer* **2010,** 51 (5), 1010-1015 DOI: https://doi.org/10.1016/j.polymer.2010.01.009.

2. Zhu, W.; Huang, X.; Li, C.; Xiao, Y.; Zhang, D.; Guan, G. High-molecular-weight aliphatic polycarbonates by melt polycondensation of dimethyl carbonate and aliphatic diols: synthesis and characterization. *Polymer International* **2011,** 60 (7), 1060-1067 DOI: 10.1002/pi.3043.

3. García-Martín, M. G.; Pérez, R. R.; Hernández, E. B.; Espartero, J. L.; Muñoz-Guerra, S.; Galbis, J. A. Carbohydrate-Based Polycarbonates. Synthesis, Structure, and Biodegradation Studies. *Macromolecules* **2005,** 38 (21), 8664-8670 DOI: 10.1021/ma050676k.

4. Rokicki, G. Aliphatic cyclic carbonates and spiroorthocarbonates as monomers. *Progress in Polymer Science* **2000,** 25 (2), 259-342 DOI: https://doi.org/10.1016/S0079-6700(00)00006-X.

5. Artham, T.; Doble, M. Biodegradation of Aliphatic and Aromatic Polycarbonates.

Macromolecular Bioscience **2008,** 8 (1), 14-24 DOI: 10.1002/mabi.200700106.

6. Pranamuda, H.; Chollakup, R.; Tokiwa, Y. Degradation of Polycarbonate by a Polyester-Degrading Strain, Amycolatopsis sp. Strain HT-6. *Applied and Environmental Microbiology* **1999,** 65 (9), 4220-4222.

7. Zhang, Z.; Kuijer, R.; Bulstra, S. K.; Grijpma, D. W.; Feijen, J. The in vivo and in vitro degradation behavior of poly(trimethylene carbonate). *Biomaterials* **2006,** 27 (9), 1741-1748 DOI: https://doi.org/10.1016/j.biomaterials.2005.09.017.

8. Zhu, K. J.; Hendren, R. W.; Jensen, K.; Pitt, C. G. Synthesis, properties, and biodegradation of poly(1,3-trimethylene carbonate). *Macromolecules* **1991,** 24 (8), 1736-1740 DOI: 10.1021/ma00008a008.

9. Meabe, L.; Lago, N.; Rubatat, L.; Li, C.; Müller, A. J.; Sardon, H.; Armand, M.; Mecerreyes, D. Polycondensation as a Versatile Synthetic Route to Aliphatic Polycarbonates for Solid Polymer Electrolytes. *Electrochimica Acta* **2017,** 237, 259-266 DOI: https://doi.org/10.1016/j.electacta.2017.03.217.

10. Sisti, L.; Totaro, G.; Marchese, P., PBS Makes its Entrance into the Family of Biobased Plastics. In *Biodegradable and Biobased Polymers for Environmental and Biomedical Applications,* Kalia, S., Avérous, L., Eds. 2016; pp 225-285.

11. van Sliedregt, A.; Knook, M.; Hesseling, S. C.; Koerten, H. K.; de Groot, K.; van Blitterswijk, C. A. Cellular reaction on the intraperitoneal injection of four types of polylactide particulates. *Biomaterials* **1992,** 13 (12), 819-824 DOI: https://doi.org/10.1016/0142-9612(92)90174-M.

12. Rücker, M.; Laschke, M. W.; Junker, D.; Carvalho, C.; Schramm, A.; Mülhaupt, R.; Gellrich, N.-C.; Menger, M. D. Angiogenic and inflammatory response to biodegradable

scaffolds in dorsal skinfold chambers of mice. *Biomaterials* **2006,** 27 (29), 5027-5038 DOI: https://doi.org/10.1016/j.biomaterials.2006.05.033.

13. Pérez-Camargo, R. A.; Meabe, L.; Liu, G.; Sardon, H.; Zhao, Y.; Wang, D.; Müller, A. J. Even–Odd Effect in Aliphatic Polycarbonates with Different Chain Lengths: from Poly (Hexamethylene Carbonate) to Poly (Dodecamethylene Carbonate). *Macromolecules* **2021**, 54 (1), 259-271 DOI: 10.1021/acs.macromol.0c02374.

14. Zhao, T.-P.; Ren, X.-K.; Zhu, W.-X.; Liang, Y.-R.; Li, C.-C.; Men, Y.-F.; Liu, C.-Y.; Chen, E.-Q. "Brill Transition" Shown by Green Material Poly(octamethylene carbonate). *ACS Macro Letters* **2015,** 4 (3), 317-321 DOI: 10.1021/acsmacrolett.5b00045.

15. Cheng, S. Z. D., Chapter 2 - Thermodynamics and Kinetics of Phase Transitions. In *Phase Transitions in Polymers*, Cheng, S. Z. D., Ed. Elsevier: Amsterdam, 2008; pp 17-59.

16. Brill, R. Über das Verhalten von Polyamiden beim Erhitzen. **1942,** 161 (1‐3), 49-64 DOI: https://doi.org/10.1002/prac.19421610104.

17. Ramesh, C.; Keller, A.; Eltink, S. J. E. A. Studies on the crystallization and melting of nylon-6,6: 1. The dependence of the Brill transition on the crystallization temperature. *Polymer* **1994,** 35 (12), 2483-2487 DOI: https://doi.org/10.1016/0032-3861(94)90367-0.

18. Yoshioka, Y.; Tashiro, K.; Ramesh, C. Structural change in the Brill transition of Nylon m/n (2) conformational disordering as viewed from the temperature-dependent infrared spectral measurements. *Polymer* **2003,** 44 (20), 6407-6417 DOI: https://doi.org/10.1016/S0032-3861(03)00593-7.

19. Tashiro, K.; Yoshioka, Y. Conformational disorder in the Brill transition of uniaxially-oriented nylon 10/10 sample investigated through the temperature-dependent measurement of X-ray fiber diagram. *Polymer* **2004,** 45 (18), 6349-6355 DOI:

https://doi.org/10.1016/j.polymer.2004.07.024.

20. Jones, N. A.; Atkins, E. D. T.; Hill, M. J. Comparison of Structures and Behavior on Heating of Solution-Grown, Chain-Folded Lamellar Crystals of 31 Even−Even Nylons. *Macromolecules* **2000,** 33 (7), 2642-2650 DOI: 10.1021/ma9919559.

21. Radusch, H. J.; Stolp, M.; Androsch, R. Structure and temperature-induced structural changes of various polyamides. *Polymer* **1994,** 35 (16), 3568-3571 DOI: https://doi.org/10.1016/0032-3861(94)90926-1.

22. Jones, N. A.; Cooper, S. J.; Atkins, E. D. T.; Hill, M. J.; Franco, L. Temperature-induced changes in chain-folded lamellar crystals of aliphatic polyamides. Investigation of nylons 2 6, 2 8, 2 10, and 2 12. **1997,** 35 (4), 675-688 DOI: https://doi.org/10.1002/(SICI)1099-0488(199703)35:4<675::AID-POLB14>3.0.CO;2-D.

23. Lotz, B. Brill Transition in Nylons: The Structural Scenario(). *Macromolecules* **2021**, 54 (2), 565-583 DOI: 10.1021/acs.macromol.0c02409.

24. Lotz, B. Original Crystal Structures of Even–Even Polyamides Made of Pleated and Rippled Sheets. *Macromolecules* **2021,** 54 (2), 551-564 DOI: 10.1021/acs.macromol.0c02404.

25. Feldman, A. Y.; Wachtel, E.; Vaughan, G. B. M.; Weinberg, A.; Marom, G. The Brill Transition in Transcrystalline Nylon-66. *Macromolecules* **2006,** 39 (13), 4455-4459 DOI: 10.1021/ma060487h.

26. Tashiro, K.; Yoshioka, Y. Molecular dynamics simulation of the structural and mechanical property changes in the Brill transition of nylon 10/10 crystal. *Polymer* **2004,** 45 (12), 4337-4348 DOI: https://doi.org/10.1016/j.polymer.2004.03.082.

27. Olmo, C.; Casas, M. T.; Martínez, J. C.; Franco, L.; Puiggalí, J. Thermally Induced Structural Transitions of Nylon 4 9 as a New Example of Even–Odd Polyamides. *Polymers* **2018,**

10 (2), 198.

28. Bertoldo Menezes, D.; Reyer, A.; Musso, M. Investigation of the Brill transition in nylon 6,6 by Raman, THz-Raman, and two-dimensional correlation spectroscopy. *Spectrochimica Acta Part A: Molecular and Biomolecular Spectroscopy* **2018,** 190, 433-441 DOI: https://doi.org/10.1016/j.saa.2017.09.055.

29. Pepin, J.; Gaucher, V.; Rochas, C.; Lefebvre, J.-M. In-situ SAXS/WAXS investigations of the mechanically-induced phase transitions in semi-crystalline polyamides. *Polymer* **2019,** 175, 87-98 DOI: https://doi.org/10.1016/j.polymer.2019.04.073.

30. Nair, S. S.; Ramesh, C.; Tashiro, K. Crystalline Phases in Nylon-11: Studies Using HTWAXS and HTFTIR. *Macromolecules* **2006,** 39 (8), 2841-2848 DOI: 10.1021/ma052597e.

31. Vasanthan, N.; Murthy, N. S.; Bray, R. G. Investigation of Brill Transition in Nylon 6 and Nylon 6,6 by Infrared Spectroscopy. *Macromolecules* **1998,** 31 (23), 8433-8435 DOI: 10.1021/ma980935o.

32. Zhao, T.-P.; Celli, A.; Ren, X.-K.; Xu, J.-R.; Yang, S.; Liu, C.-Y.; Chen, E.-Q. Sharp and strong "Brill transition" of poly(hexamethylene dithiocarbonate). *Polymer* **2017,** 113, 267-273 DOI: https://doi.org/10.1016/j.polymer.2017.02.045.

33. Berti, C.; Celli, A.; Marchese, P.; Marianucci, E.; Marega, C.; Causin, V.; Marigo, A. Aliphatic poly(alkylene dithiocarbonate)s: Thermal properties and structural characteristics of poly(hexamethylene dithiocarbonate). *Polymer* **2007,** 48 (1), 174-182 DOI: https://doi.org/10.1016/j.polymer.2006.11.035.

34. Kricheldorf, H. R.; Mahler, A. Polymers of carbonic acid 18: polymerizations of cyclobis(hexamethylene carbonate) by means of BuSnCl3 or Sn(II)2-ethylhexanoate. *Polymer* **1996,** 37 (19), 4383-4388 DOI: https://doi.org/10.1016/0032-3861(96)00288-1.

35. Arandia, I.; Meabe, L.; Aranburu, N.; Sardon, H.; Mecerreyes, D.; Müller, A. J. Influence of Chemical Structures on Isodimorphic Behavior of Three Different Copolycarbonate Random Copolymer Series. *Macromolecules* **2020**, 53(2), 669-681 DOI: 10.1021/acs.macromol.9b02078.

36. Lorenzo, A. T.; Arnal, M. L.; Albuerne, J.; Müller, A. J. DSC isothermal polymer crystallization kinetics measurements and the use of the Avrami equation to fit the data: Guidelines to avoid common problems. *Polymer Testing* **2007,** 26 (2), 222-231 DOI: https://doi.org/10.1016/j.polymertesting.2006.10.005.

37. Masubuchi, T.; Sakai, M.; Kojio, K.; Furukawa, M.; Aoyagi, T. Structure and Properties of Aliphatic Poly(carbonate) glycols with Different Methylene Unit Length. *e-Journal of Soft Materials* **2007,** 3, 55-63 DOI: 10.2324/ejsm.3.55.

38. Snyder, R. G.; Schachtschneider, J. H. Vibrational analysis of the n-paraffins—I: Assignments of infrared bands in the spectra of C3H8 through n-C19H40. *Spectrochimica Acta* **1963,** 19 (1), 85-116 DOI: https://doi.org/10.1016/0371-1951(63)80095-8.

39. Schachtschneider, J. H.; Snyder, R. G. Vibrational analysis of the n-paraffins—II: Normal co-ordinate calculations. *Spectrochimica Acta* **1963,** 19 (1), 117-168 DOI: https://doi.org/10.1016/0371-1951(63)80096-X.

40. Kobayashi, S.; Tadokoro, H.; Chatani, Y. Structural studies on polyethers, $[-(CH_2)_m-O-]_n$. VI. The higher members with m = 6–10, 12. *Die Makromolekulare Chemie* **1968,** 112 (1), 225-241 DOI: 10.1002/macp.1968.021120120